Available online at www.sciencedirect.com
ScienceDirect
Ceramics International 37 (2011) 3691–3696
CERAMICS INTERNATIONAL
www.elsevier.com/locate/ceramint

Structural, physical, magnetic and electrical properties of La-substituted W-type hexagonal ferrites

Mukhtar Ahmad [a], Faiza Aen [a], M.U. Islam [a], Shahida B. Niazi [b], M.U. Rana [a,*]

[a] *Department of Physics, Bahauddin Zakariya University, Multan 60800, Pakistan*
[b] *Department of Chemistry, Bahauddin Zakariya University, Multan 60800, Pakistan*

Received 27 April 2011; received in revised form 7 June 2011; accepted 15 June 2011
Available online 23 June 2011

Abstract

Lanthanum doped W-type hexaferrites $BaZn_2La_xFe_{16-x}O_{27}$ ($x = 0, 0.2, 0.4, 0.6, 0.8, 1.0$) were synthesized by co-precipitation and sintered at 1320 °C. The X-ray diffraction reveals W-type hexagonal structure with few traces of secondary phase. The decrease in grain size as a function of La-concentration is attributed to the fact that La acts as a grain inhibitor. The saturation magnetization and remanance decrease due to spin canting on B-sites. The increase in coercivity follows $1/r$ behavior where r is the radius of grain. The DC resistivity was observed to increase from 0.59×10^7 to 8.42×10^7 Ω cm with increasing La-contents due to the unavailability of Fe^{3+} ions. This enhancement in resistivity makes these materials promising candidates for use at high frequencies in order to reduce eddy current losses.

Keywords: W-type hexaferrites; Rare-earth substitution; X-ray diffraction; Vibrating sample magnetometry; Room temperature resistivity

1. Introduction

Hexagonal ferrites have been widely used as permanent magnets and can provide energy permanently without any recharging, as in case of a battery which needs to be recharged after a short while. These ferrites show promising properties in microwave absorption and magneto-optic or perpendicular recording media [1]. In the last decades these magnetic materials, capable of combining a high resistivity and permeability, are found in numerous products used in our daily life such as home appliances, electronic devices, communication equipments and computers [2]. In W-type barium hexagonal structure the iron ions exist on seven different sites known as $4f_{vi}$, 2d, 12k, 6g, 4f, $4f_{iv}$, and 4e [3]. An improvement in the intrinsic magnetic properties of hexaferrites can be achieved by using optimization of synthesis parameters and partially substitution for Ba or Fe sites or both. Many reports have recently shown that rare-earth (RE) substituted M-hexaferrites have exhibited improved magnetic properties [4,5]. The improvement is largely associated with the increase of magnetocrystalline anisotropy, coercive force and magnetization as observed in La-doped strontium hexaferrites [6]. Lechevallier et al. [7] and Wang et al. [5] reported the substitution of Sm ions yielding fine M-type ferrite powders resulting an increase in coercive field. Usually the rare-earth (RE) ions were substituted for Sr (Ba) or Fe, taking into accounts the ionic radii of the elements [4]. Rare earth elements (La, Sm and Nd) can also be used as inhibition agents of the grain growth mechanism at high temperature [2,4]. W-type hexagonal ferrites are of special interest because of their wide span of different applications, for example W-type ferrites $BaCo_{2-x}Zn_xFe_{16}O_{27}$ can be used as effective absorbers of electromagnetic radiations in the microwave region, non-conductive permanent magnets or as the working body of magnetic refrigerators depending upon zinc concentrations [2]. Polycrystalline W-type hexagonal ferrites are good magnetic semiconductors with low electrical conductivity as well as low eddy currents and can play an important role in various technological applications mainly in microwave absorbers [8]. The polycrystalline samples of the composition $BaZn_{2-x}Co_xFe_{16}O_{27}$ were prepared by Hemeda et al. [9]. The M–H loops for all samples clearly showed lower coercivity indicating that all the samples belong to the family of soft ferrites. The room

---

[*] Corresponding author. Tel.: +92 61 9210199; fax: +92 61 9210068.
E-mail addresses: mazharrana@bzu.edu.pk, ahmadmr25@yahoo.com (M.U. Rana).

0272-8842/$36.00 © 2011 Elsevier Ltd and Techna Group S.r.l. All rights reserved.
doi:10.1016/j.ceramint.2011.06.031

temperature electrical resistivity of a Ti doped sample of $SrCu_2Fe_{16}O_{27}$ was found to vary from 10^3 to 10^4 Ω cm [8,10]. Rezlescu et al. [11] reported the rare-earth substituted strontium ferrite nanopowders with higher values of concentration ($x = 0.2$, 0.5, 1). It was observed that an increased heat treatment was beneficial in order to eliminate the intermediate phases that can deteriorate the magnetic properties and to form single phase hexaferrites.

The aim of the present work is to synthesize La-substituted W-type hexagonal ferrites and to study their structural, magnetic and electrical properties of $BaZn_2La_xFe_{16-x}O_{27}$ powders which are not reported frequently in the literature. Also the lack of knowledge about the La-substituted W-type ferrites stimulates us to prepare and analyze $BaZn_2La_xFe_{16-x}O_{27}$ hexaferrites. Moreover the rare earth substitution was employed to inhibit the grains growth and to promote the ferritization reaction. The lanthanides also improve the mechanical materials hardness [11]. The experiments carried out by Dung et al. [12] showed that the La substitutions improve the hard magnetic properties of hexaferrite.

2. Experimental

The present samples were prepared by co-precipitation method. Analytical grade ferric chloride ($FeCl_3·6H_2O$), barium nitrate ($Ba(NO_3)_2$), zinc oxide (ZnO) and lanthanum oxide (La_2O_3) were used as starting materials for the preparation of $BaZn_2La_xFe_{16-x}O_{27}$ ($x = 0$, 0.2, 0.4, 0.6, 0.8, 1) powders. After stoichiometric calculations, the required amounts of salts were dissolved in de-ionized water. Since La_2O_3 is insoluble in water, first it was dissolved in nitric acid (HNO_3) at 80 °C to remove nitrates and then poured into the as-prepared solution. NaOH and Na_2CO_3 were used as precipitating agents to maintain pH at 9–11. The solution was stirred for 2 h; the precipitating agents were added drop wise to get the precipitates. The precipitates were washed with de-ionized water until no chloride ions were found in the solution checked by $AgNO_3$ solution. The precipitates were dried at 110 °C for 24 h in an oven and ground in an agate and mortar for 2 h. The dried powder was calcined at 1050 °C for 2 h, was again ground and then pressed into pellets under the load of (∼30 kN) using Paul-Otto Weber hydraulic press. The pellets were then finally sintered at 1320 °C for 8 h. X-ray diffraction was carried out using Shimadzu X-ray diffractometer equipped with CuKα radiation ($\lambda = 1.5406$ Å). Bulk density was measured by Archimedes's principle. The magnetic properties like saturation magnetization (M_s), remanent magnetization (M_r) and coercivity (H_c) were measured by a vibrating sample magnetometer (VSM) at room temperature. DC resistivity was measured by two probe method using a DC power supply model IP-2717 (Heath Kit) and a very sensitive electrometer model 610C (Keithly).

3. Results and discussion

3.1. Structural properties

X-ray diffraction patterns of all the compositions of La-substituted $BaZn_2La_xFe_{16-x}O_{27}$ hexaferrites are shown in Fig. 1. All peaks in XRD patterns were compared with JCPDS data and it reveals that for $x = 0$, the $BaZn_2La_xFe_{16-x}O_{27}$ ferrites are single phase W-type hexagonal ferrites while for compositions with ($x \geq 0.2$), secondary phase $LaFeO_3$ is observed. These phases were identified by using JCPDS card # 82-1958. The presence of $LaFeO_3$ phase at $x \geq 0.2$ compositions shows that La^{3+} additives did not enter totally into the BaW hexaferrites structure, and this resulted in incomplete reaction and do not form a solid solution as a result of its limited solubility.

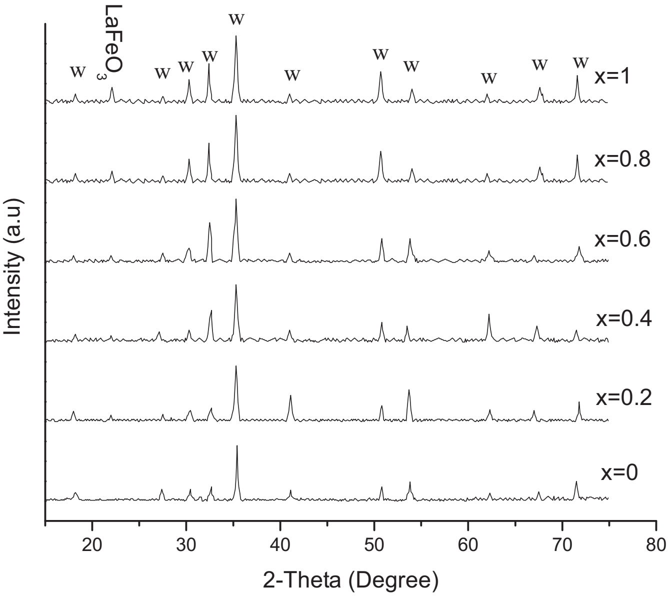

Fig. 1. X-ray diffraction patterns for $BaZn_2La_xFe_{16-x}O_{27}$ ($0 \leq x \leq 1.0$) ferrites.

The peaks were indexed and lattice parameters '*a*' and '*c*' for each concentration were calculated by the relation [13]:

$$\mathrm{Sin}^2\,\theta = \frac{\lambda^2}{3a^2(h^2+hk+k^2)} + \left(\frac{\lambda^2}{4c^2}\right)l^2 \tag{1}$$

The calculated values of '*a*' and '*c*' are listed in Table 1. It is observed from these results that the values of '*a*' and '*c*' obtained for unsubstituted sample ($x = 0$) are 5.865 Å and 33.2597 Å respectively which agree well with earlier reported values for $BaFe_{16}O_{27}$ [14]. However by substituting La^{3+}, W-type phases were developed and lattice parameters '*a*' and '*c*' are observed to be greater than those for the sample without La-substitution. This behavior can be explained on the basis of ionic radii of the substituted ions [14]. The ionic radius of La^{3+}

Table 1
Lattice parameters '*a*', '*c*', cell volume, bulk density, X-ray density and porosity of $BaZn_2La_xFe_{16-x}O_{27}$ ferrites.

x	*a* (Å)	*c* (Å)	Volume (Å^3)	*D* (g/cm^3)	D_x (g/cm^3)	%*P*
0.0	5.865	33.259	990.75	5.25	5.34	1.6
0.2	5.871	33.290	993.13	5.11	5.38	5.0
0.4	5.878	33.287	996.46	5.08	5.42	6.3
0.6	5.876	33.289	995.72	5.06	5.48	7.6
0.8	5.877	33.279	996.09	5.02	5.54	9.4
1.0	5.876	33.289	995.72	4.96	5.59	11.3

is 1.15 Å which prefers octahedral coordinated B-sites [4,15], where as in hexaferrites, Fe^{3+} ions (ionic radius = 0.67 Å) prefer to occupy three different kinds of sites (A, B and the five-fold coordination sites) [16,17]. As La is substituted, it occupies octahedral sites followed by the migration of some Fe^{3+} ions from octahedral sites to tetrahedral A-sites. Therefore with the substitution of La-contents both lattice parameters '*a*' and '*c*' are larger than the sample without substitution.

3.2. Physical properties

Density plays an important role in analyzing physical properties of magnetic ceramics. In the present samples, the Archimedes's principle was used to measure the bulk density given by the relation:

$$D = \left[\frac{W_{\mathrm{air}}}{\text{Weight loss in the liquid}}\right] \times D_{\mathrm{t}} \tag{2}$$

where W_{air} = weight of sample in air and D_{t} is the density of toluene (0.857 g/cm^3).

The X-ray density was measured by using the following relation:

$$D_{\mathrm{x}} = \frac{ZM}{N_{\mathrm{A}}V} \tag{3}$$

where $Z = 2$, number of molecules/unit cell, M = molecular weight, N_{A} = Avogadro's number (6.02×10^{23}/mole), $V = a^2c \sin 120^\circ$ (volume of the unit cell).

Finally percentage porosity of all the samples was calculated by using the formula:

$$\%P = \left(1 - \frac{D}{D_{\mathrm{x}}}\right) \times 100 \tag{4}$$

The values for bulk density (D), X-ray density (D_{x}) and porosity are listed in Table 1. The variation of bulk density, X-ray density and porosity as a function of La contents is shown in Figs. 2 and 3. It is observed that bulk density decreases by increasing La-contents. This decreasing behavior may be attributed to the reason that La has a smaller value of density (6.14 g/cm^3) as compared to that of Fe (7.8 g/cm^3). The X-ray density increases by increasing La contents because the value of atomic weight of La is 138.9 amu which is greater than that of Fe (55.85 amu). Finally porosity of the samples increases with increasing La contents due to decrease in bulk density. The results show that the bulk density is less than X-ray density due to the presence of pores created during sintering process [16].

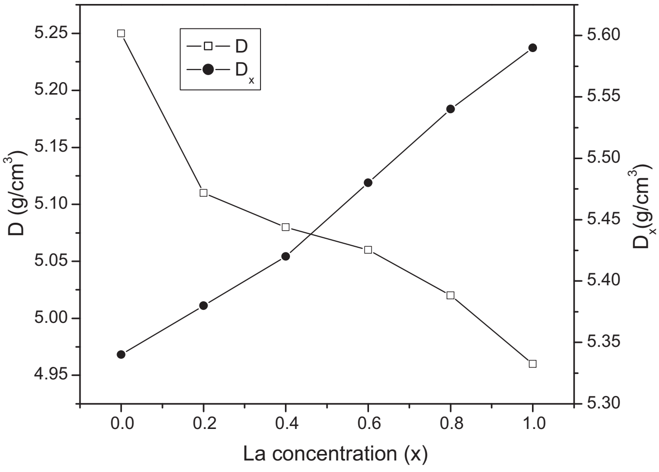

Fig. 2. Bulk density (D) and X-ray density (D_{x}) vs. La-concentration (x).

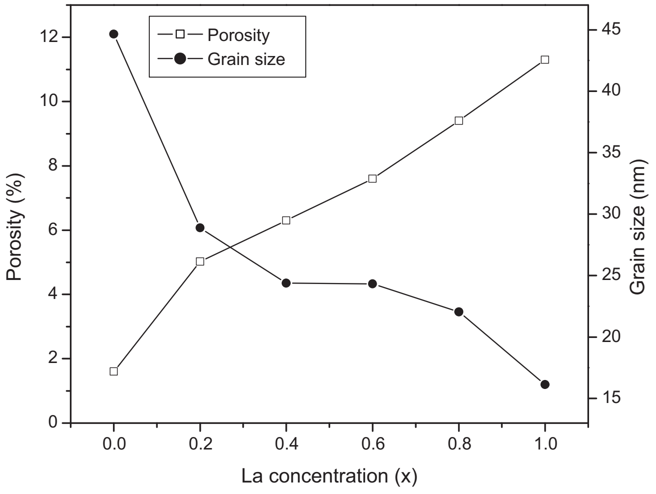

Fig. 3. Porosity and grain size vs. La-concentration (x).

3.3. Grain size measurements

The grain size for each composition was calculated from XRD patterns by using well known Debye Scherrer formula [15] given by:

$$t = \frac{0.9\lambda}{\beta \cos\theta_{\mathrm{B}}} \tag{5}$$

where λ = 1.5406 Å, β = full width at half maximum (FWHM), θ_{B} = Bragg's angle.

The variation of grain size with increasing La-concentration is shown in Fig. 3. This behavior is attributed to the fact that higher the porosity smaller is the grain size [9] and La-substitution inhibits the grain growth.

3.4. Magnetic properties

The M–H loops of all samples (x = 0, 0.2, 0.4, 0.6, 0.8, 1) are shown in Fig. 4. It can be seen from the results that coercive field $H_{\mathrm{c}} < 1$ kOe for all the compositions which reveals that the prepared ferrites have soft character. The variation of coercive field (H_{c}) with increasing La-concentration is shown in Fig. 5. Smit and Wijn [18] reported the variation of coercivity with porosity in Ni–Zn ferrites and it was reported that H_{c} increases by increasing porosity. Also higher porosity samples contain smaller crystal size which leads to high coercive field [9]. Our results show that the porosity increases with decreasing grain size measured by Scherrer formula for each sample. This confirms that H_{c} is inversely proportional to the packing of magnetic materials or the grain size. The increasing behavior of

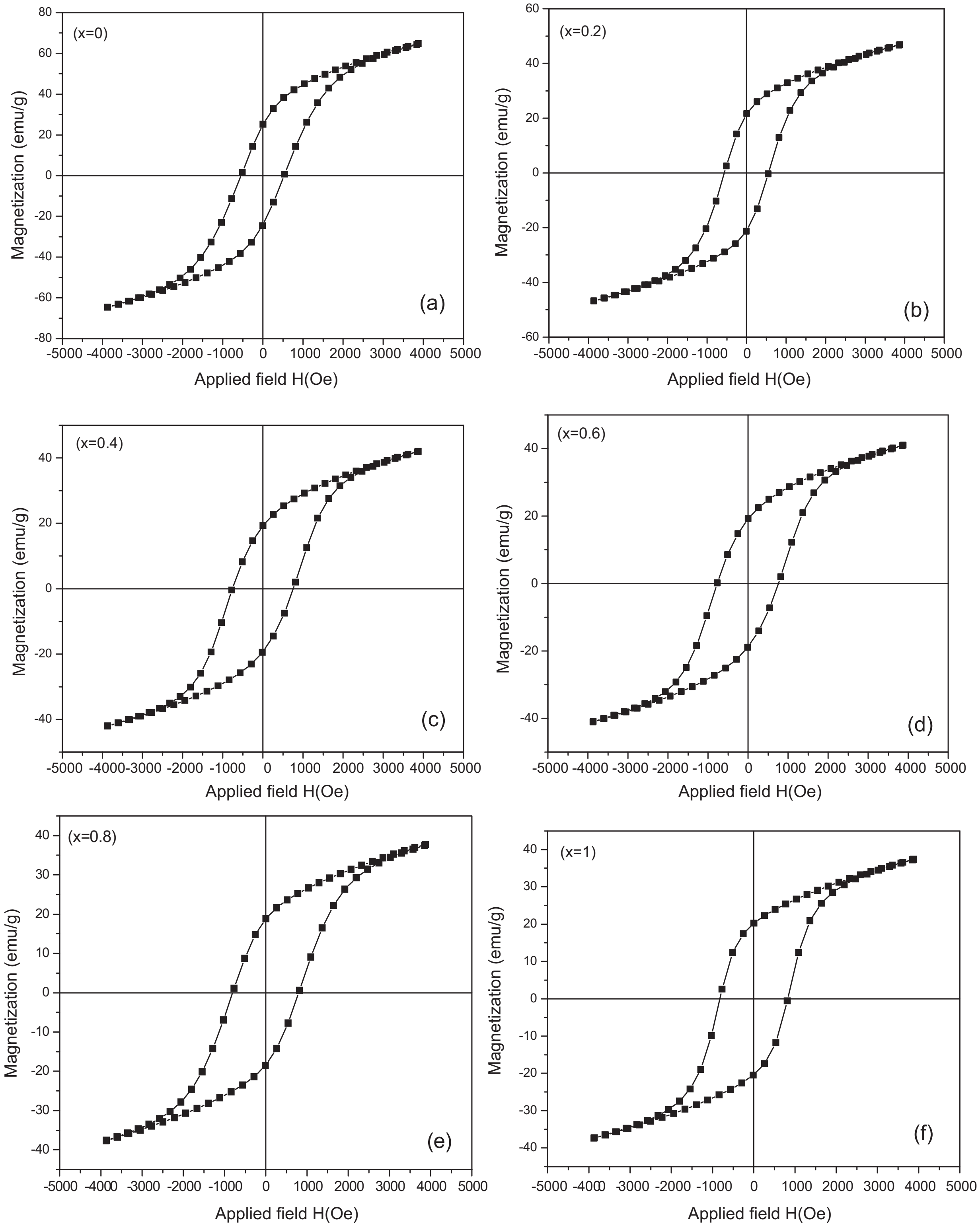

Fig. 4. (a–f) M–H loops for $BaZn_2La_xFe_{16-x}O_{27}$ ($0 \leq x \leq 1.0$) ferrites.

H_c may be due to the enhancement of the magneto-crystalline anisotropy [4,7] with anisotropic Fe^{2+} ions locating on 2a sites as usually found in rare earth ions substitution [4].

The saturation magnetization (M_s) and remanance (M_r) of $BaZn_2La_xFe_{16-x}O_{27}$ samples show a decreasing behavior with increasing La concentration as shown in Fig. 6. This behavior may be due to the difference between the ionic radii of La^{3+} and Fe^{3+} which introduces local strain that may cause the disorder and modifications of local electronic states [11]. In general the RE substitutions weaken the super exchange interactions between Fe sites because of its strongly distorted environment [11] resulting in the reduction of total magnetic moment. As La

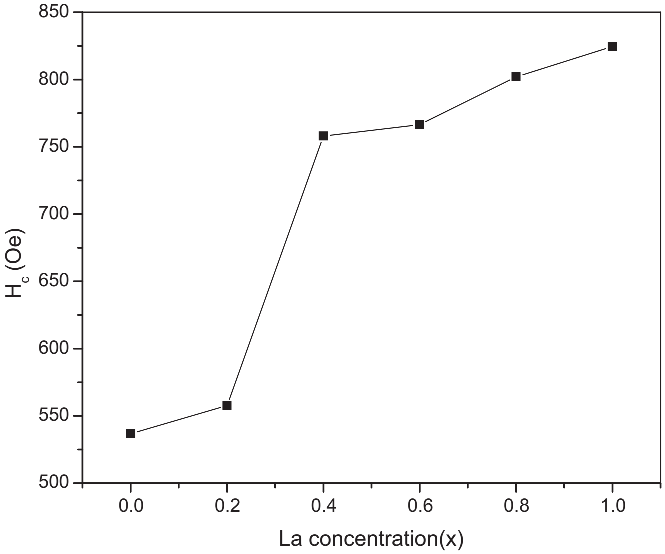

Fig. 5. Coercive force (H_c) vs. La-concentration (x).

is paramagnetic and Fe is ferromagnetic, so saturation magnetization and remanance decrease as a function of La-concentration.

Moreover spin canting phenomenon is usually caused by the rare earth ions substitution [4]. As reported by D.M. Hemeda et al, Mores et al. purposed that spin canting may originate from cationic vacancies disorder [14]. In our samples the substitution of La^{3+} for Fe^{3+} produces vacancies which reduce the M_s due to cationic redistribution during substitution [14].

3.5. Electrical resistivity

As shown in Fig. 7, the room temperature resistivity increases from a value 0.59×10^7 to 8.42×10^7 Ω cm with increasing La-concentration. Hence the present samples can be used at higher frequencies due to low eddy current losses [8]. As La ions prefer to occupy octahedral sites followed by the migration of some Fe^{3+} ions to tetrahedral sites and converting them into Fe^{2+} ions in order to maintain overall electrical neutrality. As a result Fe^{3+} ions concentration is lowered on octahedral sites: the sites responsible for conduction in ferrites. All these factors would limit the hopping probability between Fe^{3+} and Fe^{2+} ions thereby enhancing the resistivity. Moreover porosity in the investigated samples has been observed to increase so this increased number of pores in turn hinders the motion of charge carriers [19] and as a result electrical resistivity increases with increasing La-concentration. These parameters make these materials useful at high frequencies, radar absorbing materials and electromagnetic interference attenuation [8].

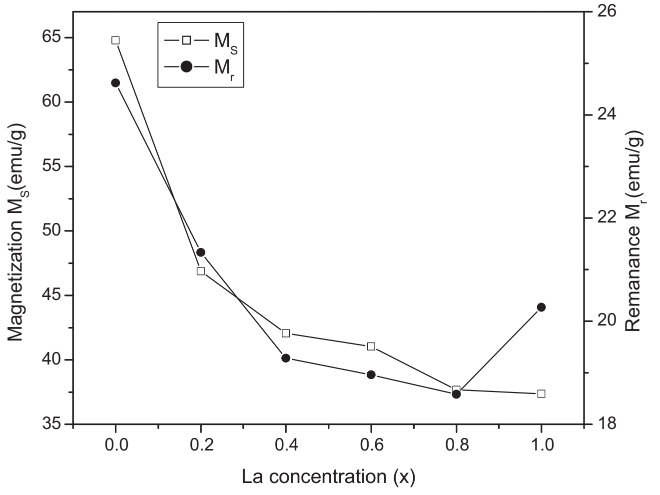

Fig. 6. Saturation magnetization (M_s) and remanance (M_r) vs. La-concentration (x).

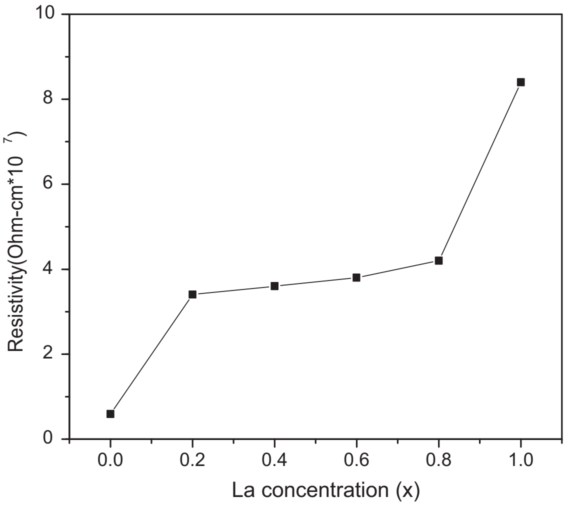

Fig. 7. Electrical resistivity vs. La-concentration (x).

4. Conclusion

Nano-metric W-type hexagonal ferrites $BaZn_2La_xFe_{16-x}O_{27}$ were obtained by co-precipitation. The coercive force follows the $H_c \propto 1/r$ (r is grain diameter) behavior and it ranges from 536 to 824 Oe as a function of La-contents. The saturation magnetization and remanance decreased by increasing La ions, as rare-earth ions weaken the super exchange interactions between A and B sites. The room temperature DC electrical resistivity increases by increasing La-contents due to increase in porosity which hinders the hoping of charge carriers. All these properties are useful to reduce the eddy current losses in the samples. From these results, it can be concluded that the investigated ferrites may be promising candidates for high frequency applications, radar wave absorbing materials (RAMs) and for electromagnetic interference (EMI) attenuation.

Acknowledgement

One of the authors (Mukhtar Ahmad) is thankful to Higher Education Commission (HEC) of Pakistan for its financial support under the indigenous PhD scholarship program for the said project.

References

[1] Z. Han, L. Dong, Z. Wu, X. Zhang, Structure of $BaLa_xFe_{12-x}O_{19}/SiO_2$ synthesized by sol–gel method, J. Rare Earths 24 (2006) 75–77.

[2] M.A. Ahmad, N. Okasha, R.M. Kershi, Could Mg content control the conduction mechanism of Ba Co Zn–W-type hexagonal ferrites? J. Magn. Magn. Mater. 321 (2009) 3967–3973.

[3] P.S. Sawadh, D.K. Kulkarni, Magnetic and electrical studies CU_2–W ferrite, Mater. Chem. Phys. 63 (2000) 170–173.

[4] S. Ounnunkad, Improving magnetic properties of barium hexaferrites by La or Pr substitution, Solid State Commun. 138 (2006) 472–475.

[5] J.F. Wang, C.B. Ponton, I.R. Harris, A study of Sm-substituted SrM magnets sintered using hydrothermally synthesized powders, J. Magn. Magn. Mater. 298 (2006) 122–131.

[6] X. Liu, W. Zhong, S. Yang, Z. Yu, B. Gu, Y. Du, Influences of La^{3+} substitution on the structure and magnetic properties of M-type strontium ferrites, J. Magn. Magn. Mater. 238 (2002) 207–214.

[7] L. Lechevallier, J.M. Le Breton, J.F. Wang, I.R. Harris, Structural analysis of hydrothermally synthesized $Sr_{1-x}Sm_xFe_{12}O_{19}$ hexagonal ferrites, J. Magn. Magn. Mater. 269 (2004) 192–196.

[8] M.J. Iqbal, R.A. Khan, Enhancement of electrical and dielectric properties of Cr doped $BaZn_2$ W-type hexaferrite for potential applications in high frequency devices, J. Alloys Compd. 478 (2009) 847–852.

[9] D.M. Hemeda, A. Al Sharif, O.M. Hemeda, Effect of Co substitution on the structural and magnetic properties of Zn–W hexaferrite, J. Magn. Magn. Mater. 315 (2007) L11.

[10] A.M. Abo El Ata, F.M. Reicha, M.M. Ali, Transport and magnetic permeability study of $SrCu_{2-x/2}Ti_xFe_{16-x}O_{27}$ W-type hexaferrites, J. Magn. Magn. Mater. 292 (2005) 17–24.

[11] N. Rezlescu, C. Doroftei, E. Rezlescu, P.D. Popa, The influence of heat-treatment on microstructure and magnetic properties of rare-earth substituted $SrFe_{12}O_{19}$, J. Alloys Compd. 451 (2008) 492–496.

[12] N.K. Dung, D.I. Minh, B.T. Cong, N. Chau, N.X. Phue, The influence of La_2O_3 substitution on the structure and properties of Sr hexaferrite, J. Phys. IV France 7 (1997) C1–C313.

[13] B.D. Cullity, Elements of X-ray Diffraction, vol. 338, 1977, p. 102.

[14] D.M. Hemeda, O.M. Hemeda, Electrical, structural, magnetic and transport properties of $Zn_2BaFe_{16}O_{27}$ doped with Cu^{2+}, J. Magn. Mater. 320 (2008) 1557–1562.

[15] J.F. Wang, C.B. Ponton, I.R. Harris, A study of Pr-substituted strontium hexaferrite by hydrothermal synthesis, J. Alloys Compd. 403 (2005) 104–109.

[16] M.A. Ahmed, N. Okasha, M. Oaf, R.M. Kershi, The role of Mg substitution on the microstructure and magnetic properties of Ba Co Zn W-type hexagonal ferrites, J. Magn. Magn. Mater. 314 (2007) 128–134.

[17] K.J. Standly, Oxide Magnetic Materials, Clarendon Press, Oxford, 1962.

[18] J. Smit, H.P.J. Wijn, Adv. Electron. Electron Phys. 6 (1954) 69.

[19] A.A. Sattar, H.M. El-sayed, K.M. El-Shokofy, M.M. el-Tabey, The effect of Al-substitution on structure and electrical properties of Mn–Ni–Zn ferrites, J. Mater. Sci. 40 (2005) 4873–4879.